DOI: 10.1002/chem.200901758

Structure of the Complex of $[Ru(tpm)(dppz)py]^{2+}$ with a B-DNA Oligonucleotide—A Single-Substituent Binding Switch for a Metallo-Intercalator

Philip Waywell,[a, b] Veronica Gonzalez,[a] Martin R. Gill,[a] Harry Adams,[a] Anthony J. H. M. Meijer,*[a] Mike P. Williamson,*[b] and James A. Thomas*[a]

Abstract: We report the synthesis of three new complexes related to the achiral $[Ru(tpm)(dppz)py]^{2+}$ cation (tpm = tripyridazole methane, dppz = dipyrido[3,2-*a*:2′,3′-*c*]phenazine, py = pyridine) that contain an additional single functional group on the monodentate ancillary pyridyl ligand. Computational calculations indicate that the coordinated pyridyl rings are in a fixed orientation parallel to the dppz axis, and that the electrostatic properties of the complexes are very similar. DNA binding studies on the new complexes reveal that the nature and positioning of the functional group has a profound effect on the binding mode and affinity of these complexes. To explore the molecular and structural basis of these effects, circular dichroism and NMR studies on $[Ru(tpm)(dppz)py]Cl_2$ with the octanucleotides $d(AGAGCTCT)_2$ and $d(CGAGCTCG)_2$, were carried out. These studies demonstrate that the dppz ligand intercalates into the G^2–A^3 step, with {Ru(tpm)py} in the minor groove. They also reveal that the complex intercalates into the binding site in two possible orientations with the pyridyl ligand of the major conformer making close contact with terminal base pairs. We conclude that substitution at the 2- or 3-position of the pyridine ring has little effect on binding, but that substitution at the 4-position drastically disrupts intercalative binding, particularly with a 4-amino substituent, because of steric and electronic interactions with the DNA. These results indicate that complexes derived from these systems have the potential to function as sequence-specific light-switch systems.

Keywords: DNA · intercalation · luminescence · N ligands · NMR spectroscopy · ruthenium

Introduction

Small molecules that bind to DNA have a variety of possible applications including pharmaceuticals, tools for molecular biology, probes for energy and/or electron transfer, or even gene modulators.[1] In this context, over the last three decades, complexes of d^6 metal centers such as Re^I, Rh^{III}, Os^{II}, and particularly Ru^{II} have received a considerable amount of attention.[2] Due to its very interesting photophysical properties, one of the most studied systems has been the DNA intercalating complex $[Ru(bpy)_2(dppz)]^{2+}$ (dppz = dipyrido[3,2-*a*:2,3-*c*]-phenazine, bpy = 2,2′-bipyridine, Figure 1).

In aqueous solution this "DNA light-switch" complex, and its 1,10-phenanthroline analogue, display virtually no luminescence, but when bound to DNA, emission is enhanced by several orders of magnitude.[1,2] Although it is well established that the "bright state" of this effect involves the triplet $Ru^{II} \rightarrow \pi^*$(dppz) metal-to-ligand charge transfer (MLCT) manifold, the nature of the "dark state" is still under debate.[3,4] Transient spectroscopy studies reported by Olson et al. indicated that the emissive MLCT state is rapidly deactivated ($\approx$3 ps) in water.[3] They ascribed this effect to deactivation of the emissive MLCT via a second excited state that becomes lower lying in water and described this second state, which has a very low emission quantum yield, as also

[a] P. Waywell, V. Gonzalez, M. R. Gill, H. Adams, Dr. A. J. H. M. Meijer, Dr. J. A. Thomas
Department of Chemistry, University of Sheffield
Sheffield S3 7HF (UK)
Fax: (+44) 114-273-8673
E-mail: james.thomas@sheffield.ac.uk
a.meijer@sheffield.ac.uk

[b] P. Waywell, Prof. M. P. Williamson
Department of Molecular Biology and Biotechnology
University of Sheffield, Sheffield S10 2TN (UK)
Fax: (+44) 114-222-2800
E-mail: m.williamson@sheffield.ac.uk

Supporting information for this article is available on the WWW under http://dx.doi.org/10.1002/chem.200901758.

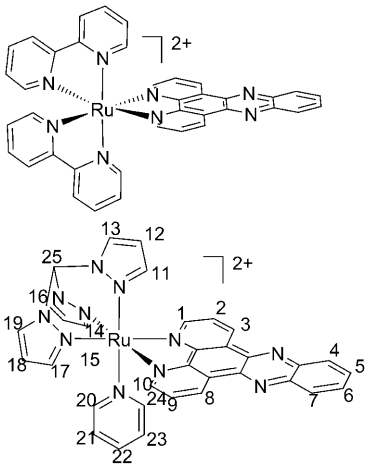

Figure 1. The structures of $[Ru(bpy)_2(dppz)]^{2+}$ (top) and [Ru(tpm)-(dppz)py]$^{2+}$ (bottom). The 3-NH_2 and 4-NH_2 derivatives have amino groups added at the positions labeled 21 and 22 respectively, while the 4-Me derivative has a CH_3 group attached at position 22.

MLCT in character. This study, and subsequent work by others,[4] supported the hypothesis that this reversal of states is due to enhanced hydrogen-bonding to the transiently reduced ligand in the second MLCT state. An alternative explanation was provided by Brennaman et al.,[5] whose work on the temperature dependence of the light switch in protic and aprotic solvents suggested that while the dark state is always the lower energy state in any solvent, the light state is preferentially populated in polar solvents due to entropic factors. Subsequently, a comprehensive theoretical study proposed that the dark state observed by Brennaman et al. was in fact a low-lying ligand-centered triplet state located on the coordinated dppz ligand, and is distinct from the low quantum yield state observed in water.[6]

When bound to DNA, $[Ru(phen)_2(dppz)]^{2+}$ and related complexes display two different luminescence decay rates. Barton and colleagues have suggested that this is due to two different binding geometries in equilibrium: a side-on mode in which the long axis of the phenazine lies approximately along the long axis of the base pair, and a second intercalative mode with the phenazine axis along the DNA dyad axis.[2] Based on NOEs observed between an adenosine H8 and a dppz proton,[7,8] displacement by a major groove binder,[9] and luminescence studies,[10] they have also suggested that the complexes bind from the major groove side.

By contrast, through studies involving binding to T4 DNA[11] and to triplex DNA,[12] the Nordén group provided evidence that the same complex intercalates from the minor groove with the suggestion that the DNA axis is bent as a consequence of the intercalation.[13] NMR studies from the groups of Aldrich-Wright and Collins based on the observation of a number of NOEs also support the minor groove binding model, both for the shorter $[Ru(phen)_2dpq]^{2+}$ complex[14–16] (dpq = dipyrido[3,2-*a*:2,3-*c*]-quinoxaline) and for $[Ru(Me_2bpy)_2(dppz)]^{2+}$ (Me_2bpy = 4,4-dimethyl-2,2-bipyridine).[17] These authors further suggested that the NOEs observed by Dupureur and Barton[7,8] may have been real but misleading, accounting for the discrepancy in the reported geometry. Many other papers have also indicated that these complexes possess several DNA binding modes.[8,10,11,14,15,18] It has even been suggested that $[Ru(phen)_2(dppz)]^{2+}$ can also bind in a non-intercalative mode,[19] in a manner similar to $[Ru(phen)_3]^{2+}$.

Clearly, there is still some ambiguity as to the binding geometry of the complexes, which constitutes a significant barrier to further development of these metallo-intercalators as therapeutic agents, as footprinting agents, and as probes of conformational change and electron transfer within the DNA double helix. The problem is exacerbated by the chirality of $[Ru(phen)_2(dppz)]^{2+}$, as each of the two enantiomers binds with two distinct lifetimes[20] and also different stoichiometries.[21] To address some of these problems, we are studying achiral intercalators such as [Ru(tpm)(dppz)py]$^{2+}$ (Figure 1, tpm = tris(pyrazolyl)methane, py = pyridine). Although binding of this complex to DNA can lead to two possible intercalative binding geometries—defined by the orientation of the pyridine ligand with respect to the duplex, vide infra—it offers distinctive synthetic advantages over the $[Ru(phen)_2(dppz)]^{2+}$ system.

One possible strategy to modulate the binding properties of such metallo-intercalators involves the addition of hydrogen bonding motifs. Indeed, it has been established that the binding preferences of $[Rh^{III}(phi)]$ systems (phi = 9,10-phenanthrenequinone diimine) can be tuned by such effects.[22] However, although sequence selective binding has been obtained by appending $[Ru(phen)_2(dppz)]^{2+}$ to specific oligonucleotides,[23] attempts to develop derivatives that intrinsically show sequence or structural binding preferences have been hampered by the fact that the cation is a coordinatively inert chiral complex of a classically inert metal center; thus if specific derivatives of the complex are required, the demands on synthesis and separation rapidly increase. Addition of a single functional group, R, onto the auxiliary phen ligands of the cation leads to two isomers, each of which is an enantiomeric pair—indeed, if R is itself chiral, then inclusion of this single functional group can lead to eight different possible structures. Using the [Ru(tpm)(dppz)] unit, and other achiral building blocks,[24] we are developing a more facile modular approach to the construction of DNA binders which surmounts these problems.

Herein we report initial results on the syntheses of complexes with potentially mixed recognition motifs, containing both intercalative and hydrogen-bond units. In this initial study, we restrict ourselves to studying the effect that the addition of a single amine unit has on the binding properties of $[Ru(tpm)(dppz)(py)]^{2+}$. To carry out this study three new complexes, $[Ru(tpm)(dppz)(3\text{-}NH_2py)]^{2+}$, $[Ru(tpm)(dppz)(4\text{-}NH_2py)]^{2+}$, and $[Ru(tpm)(dppz)(4\text{-}Mepy)]^{2+}$ (Figure 1), have been synthesized and their DNA binding properties are compared to the parent complex using a variety of biophysical techniques. We find that the change of a single substituent can modulate DNA binding and even "switch off" intercalation.

To understand the structural basis for these binding differences, an NMR study of $[Ru(tpm)(dppz)py]^{2+}$ with two double-stranded symmetrical DNA oligonucleotides, d-$(AGAGCTCT)_2$ and d$(CGAGCTCG)_2$, has been carried out, which reveals that the complex intercalates into the minor groove at the G^2–A^3 step. A calculated structure based on a limited number of NOEs reveals specific contacts between the ruthenium-bound ancillary ligands and the DNA. A consideration of this model and theoretical calculations on the complexes explains their divergent binding characteristics.

Results

The new complexes were characterized by NMR and mass spectrometry as well as elemental analysis. Additionally the structure of the $[Ru(tpm)(dppz)(3\text{-}NH_2py)]^{2+}$ ion was further confirmed by x-ray crystallography.

X-ray crystallographic study: A summary of the crystallographic data, bond lengths and bond angles for $[Ru(tpm)(dppz)(3\text{-}NH_2py)][PF_6]_2$, as well as a diagram containing thermal ellipsoids, are available as in the Supporting Information. The structure, Figure 2, contains two independent

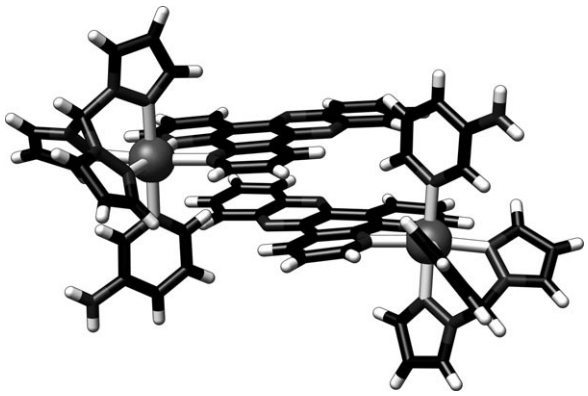

Figure 2. The two independent cations from the $2[Ru(tpm)(dppz)(3\text{-}NH_2py)](PF_6)_4]\cdot 4MeCN\cdot H_2O$ crystallographic structure.

cations. Each ruthenium center takes up a somewhat distorted octahedral coordination geometry, with the *trans* angles at the Ru^{II} centers varying between 174.9–176.8° and 172.6–177.6° respectively. The Ru–N bond lengths involving the tpm ligand vary between 2.06(1)–2.077(8) Å and 2.04(1)–2.08(1) Å, respectively, while the distances for the Ru–dppz bonds (2.04(1)–2.07(1) Å) and the Ru–N bonds involving 3-NH_2py (2.056(8) and 2.079(8) Å) are also very similar. The bite angle of the dppz is 79.9(3)°, and the bite angles for the tpm are 84.7(4), 84.3(4) and 87.8(4)°. A notable feature of each cation is the alignment of the plane of the monodentate pyridyl based ligand parallel to the long axis of the dppz ligand, vide infra.

Photophysical studies: The photophysical properties of the three new complexes are summarized in Table 1 and compared to those previously reported for $[Ru(tpm)(dppz)(py)]^{2+}$.[24] UV/Vis spectra recorded in acetonitrile are dominated by intense bands between 270–370 nm corresponding to $\pi\rightarrow\pi^*$ transitions for the aromatic nitrogen donor ligands and high-energy MLCTs involving dppz. Between 400–500 nm lower intensity bands, typical of $Ru(d\pi)\rightarrow dppz(\pi^*)$ ^{1}MLCT transitions are observed; excitation into this band results in luminescence centered around 600–660 nm that is characteristic of the {Ru(dppz)} moiety.

DFT calculations: Calculations were carried out on all four relevant $[Ru(tpm)(dppz)(L)]^{2+}$ systems, and resulted in the minimum energy structures given in Figure 3. For each of the four compounds studied, the minimum energy configuration is similar to that seen for the two independent cations of $[Ru(tpm)(dppz)(3\text{-}NH_2py)]^{2+}$ in the crystal structure, with the plane of the L ligand parallel to the long axis of the

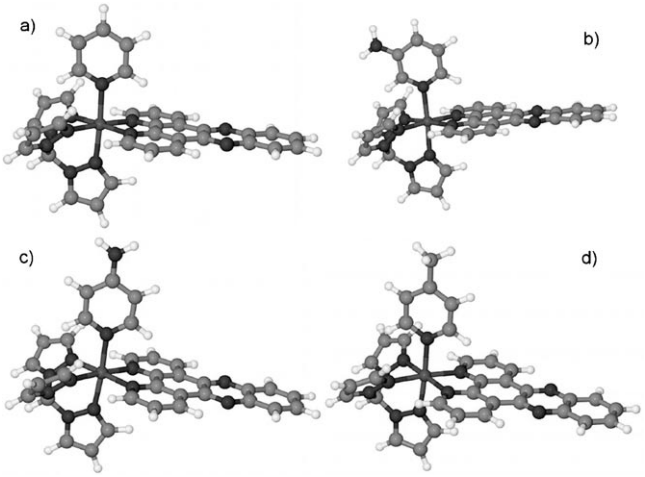

Figure 3. The four minimum energy structures of the molecules studied. a) $[Ru(tpm)(dppz)(py)]^{2+}$, b) $[Ru(tpm)(dppz)(3\text{-}NH_2py)]^{2+}$, c) $[Ru(tpm)(dppz)(4\text{-}NH_2py)]^{2+}$, and d) $[Ru(tpm)(dppz)(4\text{-}Mepy)]^{2+}$.

Table 1. Details of absorption and steady-state emission spectra of complexes.[a]

Complex	Absorption spectra λ [nm] ($10^{-3}\,\varepsilon$ [$M^{-1}cm^{-1}$])	Emission spectra λ_{em} [nm] ($\lambda_{ex}=425$ nm)
$[Ru(tpm)(dppz)(py)]^{2+}$	277 (62.5), 312 (22.3), 351 (22.7), 398 (9.1), 484 sh	616
$[Ru(tpm)(dppz)(3\text{-}NH_2py)]^{2+}$	278 (56.6), 348 (19.1), 415 (7.0), 501 sh	615
$[Ru(tpm)(dppz)(4\text{-}NH_2py)]^{2+}$	276 (72.9), 349 (19.8), 367 (16.7), 411 (9.6), 501 sh	603
$[Ru(tpm)(dppz)(4\text{-}CH_3py)]^{2+}$	276 (59.9), 348 (22.7), 411 (8.6), 490 sh	660

[a] In MeCN, at room temperature.

dppz ligand. This conclusion was confirmed by a frequency analysis. We then investigated how free L was to rotate away from this position. To elucidate this question, we calculated the stationary points for rotation around the Ru–N bond for each of the four compounds. In particular, we calculated the energy of the perpendicular conformation and the transition state between the parallel and perpendicular conformations. These energies are given in Table 2 relative

Table 2. Energetics of rotation around the Ru–N bond for the coordinated ligands of $[Ru(tpm)(dppz)(L)]^{2+}$.

L	Perpendicular conf. [kJ mol^{-1}]	Transition state [kJ mol^{-1}]
py	18.4	19.6
3-NH_2py	18.5	19.5
4-NH_2py	17.8	18.7
4-CH_3py	17.8	18.9

to the minimum energy (parallel) conformation. The perpendicular conformations were confirmed to be minima by frequency analysis. The transition states all had only a single imaginary frequency and were all situated approximately halfway between the parallel and perpendicular configuration. In all cases this state was confirmed to be associated with the Ru–N torsion through visual inspection. If one assumes Boltzmann statistics and taking into account the position of the transition state, these results mean that, for each of these complexes, less than 0.1 % will be in the perpendicular geometry and most complexes will be in a configuration close to the parallel one.

It should be pointed out that these calculations are performed in vacuo: including solvent into the calculations lowers the perpendicular configurations to approximately 14.6 and 13.5 kJ mol^{-1} above the parallel conformation for the 4-NH_2py and 3-NH_2py cases, respectively. However, it should be noted (as mentioned in the Experimental Section) that these numbers correspond to a calculation with an unconverged geometry. Nevertheless, even in the latter case, less than 0.5 % of the molecules will be in the perpendicular conformation.

The electrostatic potential (ESP) for each of the four compounds was also calculated (Figure 4). As is clear from this figure, the charge distribution across the molecule is uniform with only a difference of 0.1 between the maximum and minimum electrostatic potential. Moreover, each molecule is positively charged over its entire surface, which will lead to an attractive interaction with any neighboring negative charges.

The rigidity of the NH_2–py and CH_3–py bonds with respect to torsional motion was also investigated. Here, a clear difference between the NH_2py and 4-CH_3py systems is found. The torsional barrier for 4-CH_3-py rotation is only 10.5 J mol^{-1}. This indicates that the methyl group of $[Ru(tpm)(dppz)(4\text{-Mepy})]^{2+}$ is effectively a free rotor.

In contrast, the torsional barrier around the 4-NH_2–py bond is 70.6 kJ mol^{-1}, indicating that the amino group of $[Ru(tpm)(dppz)(4\text{-}NH_2py)]^{2+}$ is essentially rigid and cannot

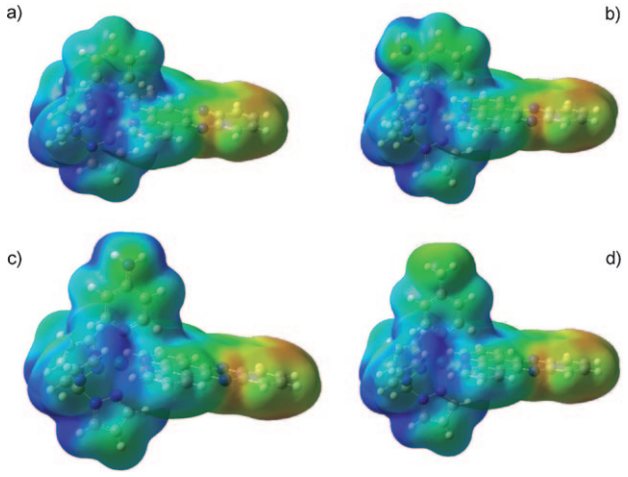

Figure 4. The electrostatic potential mapped onto the electron density for the four complexes. Density contour is 0.0004. Minimum ESP 0.1 (red). Maximum ESP 0.2 (blue). a) $[Ru(tpm)(dppz)(py)]^{2+}$, b) $[Ru(tpm)(dppz)(3\text{-}NH_2py)]^{2+}$, c) $[Ru(tpm)(dppz)(4\text{-}NH_2py)]^{2+}$, and d) $[Ru(tpm)(dppz)(4\text{-Mepy})]^{2+}$.

change its relative orientation: the flat NH_2 unit is held in the same plane as the pyridine ring parallel to the long axis of the dppz ligand. This is consistent with a large contribution from the quinoidal resonance form for coordinated 4-NH_2py and also the electrostatic calculations, which indicate that the lone pair of the amino group is not specifically located on the nitrogen.

Although the torsional barrier around the 3-NH_2–py bond of $[Ru(tpm)(dppz)(3\text{-}NH_2py)]^{2+}$ is lower than that for the 4-NH_2Py complex (41.7 kJ mol^{-1}), this value still indicates that rotation around the 3-NH_2–py bond is restricted; this conclusion is consistent with the crystal structure of the $[Ru(tpm)(dppz)(3\text{-}NH_2py)]^{2+}$ ion (Figure 2), in which the planar 3-NH_2py unit is indeed seen to be parallel to the long axis of the dppz ligand.

DNA binding studies

Equilibrium binding titrations: Water-soluble chloride salts of the two new complexes were obtained by means of anion metathesis of their respective PF_6^- salts using [*n*Bu_4N]Cl in acetone. Initially, their interaction with calf thymus (CT)-DNA in aqueous buffer (25 mM NaCl, 5 mM tris, pH 7.0) was investigated using UV/Vis spectroscopic titrations and compared to the data for $[Ru(phen)_2(dppz)]^{2+}$ and $[Ru(tpm)(dppz)(py)]^{2+}$. Addition of CT-DNA to solutions of both complexes results in hypochromicity in both MLCT and $\pi\rightarrow\pi^*$ absorption bands. Curves constructed from these absorption changes demonstrate that saturation binding has taken place. Fits of the nonlinear Scatchard plots constructed from these data using the McGhee-von Hippel model[25] led to the data summarized in Table 3.

An inspection of the data obtained indicates that although the 3-NH_2py complex has a binding affinity that is comparable with those of the parent complex, that of the 4-Mepy

Table 3. Selected binding parameters with CT-DNA.

Complex	Absorption titrations		Luminescence titrations	
	K_b [$dm^3 mol^{-1}$]	Site size S	K_b [$dm^3 mol^{-1}$]	Site size S
$[Ru(tpm)(dppz)(py)]^{2+}$[a]	5.17×10^6	3.4	4.73×10^6	3.9
$[Ru(tpm)(dppz)(3\text{-}NH_2py)]^{2+}$	5.7×10^6	1.7	4.4×10^6	1.5
$[Ru(tpm)(dppz)(4\text{-}Mepy)]^{2+}$	1.07×10^6	1.2	1.07×10^6	1.5
$[Ru(tpm)(dppz)(4\text{-}NH_2py)]^{2+}$	6.2×10^5	1.3	–[b]	–[b]

[a] Data from reference [24a]. [b] No luminescence observed.

complex is reduced by around five times, while the affinity of $[Ru(tpm)(dppz)(4\text{-}NH_2py)]^{2+}$ is almost an order of magnitude lower than the parent system and is comparable to values obtained for non-intercalating metal complexes such as the groove binding cation, $[Ru(phen)_3]^{2+}$.[26] To investigate this apparent anomaly further, luminescent titrations were carried out.

Again, luminescent titrations with $[Ru(tpm)(dppz)(3\text{-}NH_2py)]^{2+}$ and $[Ru(tpm)(dppz)(4\text{-}Mepy)]^{2+}$ show that that they display the expected light-switch effect. Fits to the saturation binding curves derived from these luminescence changes lead to estimated binding parameters (Table 3) that are comparable with data obtained from absorption titrations, again indicating that the latter complex binds with a comparatively lower affinity. However, in analogous experiments with $[Ru(tpm)(dppz)(4\text{-}NH_2py)]^{2+}$, no emission was observed even after addition of large excesses of CT-DNA. Although light-switch effects have been observed for non-intercalating systems,[27] a dppz moiety well protected from bulk aqueous solvent is a requisite for the bright state to "switch on", indicating that the interaction of $[Ru(tpm)(dppz)(4\text{-}NH_2py)]^{2+}$ with CT-DNA is not through intercalation. To definitively resolve this issue viscosity experiments were carried out.

Viscosity studies: Intercalation between base pairs increases the contour length of short rodlike DNA sequences. Consequently, intercalators induce an increase in the relative viscosity of DNA solutions, whereas classical groove binders such as netropsin—which do not lengthen the DNA helix—have no effect on relative viscosity.[26,28]

The effect of the new complexes on the viscosity of short-length CT-DNA produced by sonication is depicted in Figure 5. While the complex $[Ru(tpm)(dppz)(4\text{-}Mepy)]^{2+}$ produces very large positive viscosity changes, a lower increase is observed for the $[Ru(tpm)(dppz)(3\text{-}NH_2py)]^{2+}$ ion; nevertheless these latter changes are comparable to those observed for $[Ru(tpm)(dppz)(py)]^{2+}$ and related complexes,[24e] indicating that both these complexes intercalate into the duplex. In contrast, it is clear that addition of $[Ru(tpm)(dppz)(4\text{-}NH_2py)]^{2+}$ produces no increase in viscosity and is similar in its effect to that of the established minor groove binder H33258. These data confirm that, surprisingly, $[Ru(tpm)(dppz)(4\text{-}NH_2py)]^{2+}$ is not an intercalator. In an attempt to understand the molecular basis of the surprising change in binding mode, we probed the binding geometry of the parent complex $[Ru(tpm)(dppz)(py)]^{2+}$ with DNA using CD and NMR experiments.

Circular dichroism: Following the procedures described elsewhere,[29] $[Ru(tpm)(dppz)(py)]^{2+}$ was titrated into 1.3 mM $d(AGAGCTCT)_2$ and $d(CGAGCTCG)_2$ solutions, up to a ratio of just greater than 1:1. The high nucleotide concentration was necessary to ensure complete duplex formation, while the endpoint was determined by saturation of the detector. DNA has no CD signal in the range 320–500 nm and, since $[Ru(tpm)(dppz)(py)]^{2+}$ is achiral, it has no CD signal at all. However, on intercalation into the oligonucleotide, an induced CD (ICD) signal for the complex is generated. Two ICD bands are observed, one positive and one negative (Figure 6).

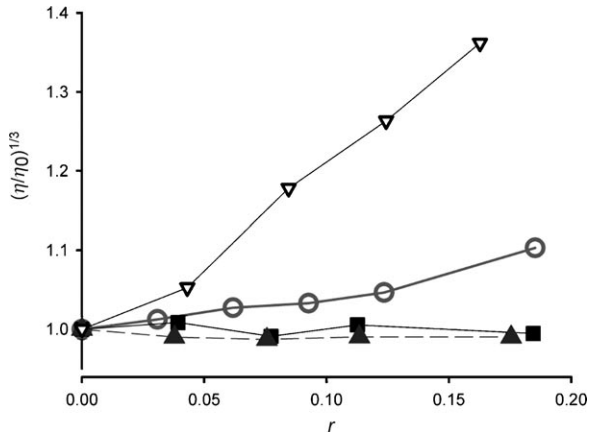

Figure 5. Plot of relative viscosity $(\eta/\eta_0)^{1/3}$ of CT-DNA versus r (r=[complex]/[DNA]) upon addition of $[Ru(tpm)(dppz)(3\text{-}NH_2py)]^{2+}$ (○), $[Ru(tpm)(dppz)(4\text{-}Mepy)]^{2+}$ (▽), $[Ru(tpm)(dppz)(4\text{-}NH_2py)]^{2+}$ (▲), and H33258 (■), a known minor groove binder, in a tris buffer (5 mM Tris, 25 mM NaCl), at pH 7.

The positive band, centered at 406 nm, corresponds to the observed metal-to-ligand charge transfer in water, a transition that is orientated along the long axis of the dppz.[13,30,31] The positive nature of this band indicates that the long axis of the dppz is orientated in an orthogonal manner in relation to the long axis of the DNA base pairs. This would suggest that the dppz is threaded through the base-pair stack and therefore the metallo-intercalator is bound in a classical intercalative mode. The negative band, centered at 352 nm, largely corresponds to a π–π^* transition residing on the dppz. The exact orientation of this transition is difficult to deduce. However, the HOMO and LUMO between which the transition occurs are positioned such that the transition itself could be parallel to the long axis of the DNA base pair in the bound complex, hence the negative ICD band. Thus, the ICD confirms the intercalatory mode and indicates

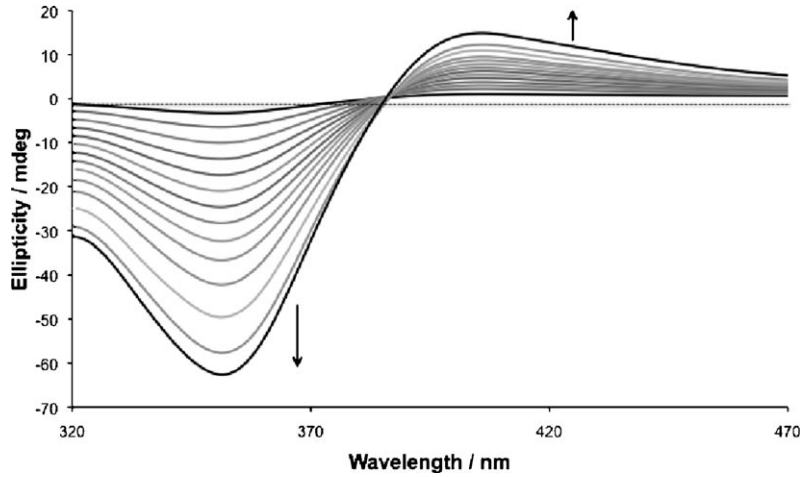

Figure 6. Circular dichroism spectra produced during the stepwise addition of $[Ru(tpm)(dppz)(py)]^{2+}$ to $d(CGAGCTCG)_2$. Similar data were obtained for $d(AGAGCTCT)_2$.

that the dppz is intercalated in a classical head-on manner, approximately orthogonal to the long axis of the base pairs.

NMR binding studies: So far, there have been no crystal structures of ruthenium-based intercalators with DNA, and the most detailed information on binding geometry has come from NMR spectroscopy, as discussed above. Previous attempts to study binding of {Ru(dppz)} systems to DNA by NMR spectroscopy have encountered difficulties due to intermediate rate exchange broadening.[7,8,17] The usual solution to this problem is either to go down in temperature, which brings some resonances into slow exchange but leads to further line broadening,[7,8] or to go up in temperature, which produces sharper lines but runs the risk of dissociating the DNA duplex before all signals can be sharpened.[17] In our studies, the increases in linewidth at low temperature prevented observation of any useful NOEs, and therefore a temperature of 308 K was used. The most important parameter for maintaining the DNA as a duplex was the concentration of the oligonucleotide, which was 2 mM duplex in all experiments.

NMR spectra of free $d(AGAGCTCT)_2$ and $d(CGAGCTCG)_2$ were assigned by using standard ^1H homonuclear 2D methods[32] as described elsewhere,[29] while the spectrum of the ligand was assigned using ^1H COSY, TOCSY and NOESY. Titration of ligand into the nucleotide solutions gave gradual chemical shift changes. At a 1:1 ratio of ligand to duplex, a single set of resonances was observed for both the ligand and the self-complementary duplex, implying that the off-rate is fast enough to lead to averaging of chemical shifts. A small number of intermolecular NOEs could be observed, but the large linewidth of the ligand meant that assignments could not be made with any confidence. Further addition of $[Ru(tpm)(dppz)(py)]^{2+}$ was therefore conducted, up to a 2:1 ratio of metal complex to duplex, and thus a 1:1 ratio of ligand to binding site assuming an asymmetric off-center intercalation position. By contrast to the quaternised dqdppn ligand (for which addition of the second equivalent led to further broadening and binding at multiple sites as described[29]) the 2:1 complex gave sharper signals, which permitted the assignment of nucleotide and ligand. Chemical shift assignments have been submitted to BioMagResBank.[33]

Twelve intermolecular NOEs were observed and assigned for the complex with $d(AGAGCTCT)_2$ (Supporting Information), while 27 were assigned for the $d(CGAGCTCG)_2$ complex (Figure 7).

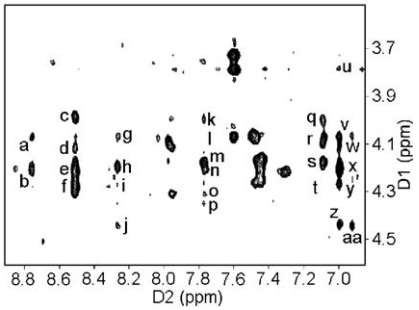

Figure 7. A selected region from the 2D ^1H NOESY spectrum of the 2:1 complex formed by $[Ru(tpm)(dppz)(py)]^{2+}$ and $d(CGAGCTCG)_2$. This region contains several intermolecular NOE contacts (labelled a–aa), some of which are at contour levels below those used for the figure. The assignments of these contacts are given in the Supporting Information.

The NOEs are all from tpm and pyridine to 4' and 5′/5" protons, and therefore clearly indicate minor groove binding. No NOEs could be assigned for protons in the dppz system, because of line broadening caused by its intercalation. There are NOEs to protons on all base pairs, but inspection shows that the majority, particularly from the equatorial ruthenium ligands, are to the G^2–A^3/T^6–C^7 base pairs, while most of the NOEs from the pyridine axial ligand are to the terminal base pair or G^2–A^3, and most of the NOEs from the tpm axial ligand are to the G^4–C^5 base pair, for both nucleotides. The data thus indicate that the dppz is intercalated in the G^2–A^3 step, with the pyridine axial ligand pointing toward the terminal base pairs and the tpm axial ligand pointing toward the center of the duplex in the major bound conformation. However, for both complexes there are NOEs that clearly do not fit this orientation, and require a structure in which the intercalation is still at the G^2–A^3 step, but the ligand is rotated by 180° so that the pyridine now points toward the center of the duplex. In the $d(AGAGCTCT)_2$ complex there is an NOE from the pyridine

ring to G^4, while in the $d(CGAGCTCG)_2$ complex, five of the observed NOEs are consistent only with this inverted geometry. This suggests that although both geometries are present in equilibrium, the preferred geometry is with the pyridine pointing toward the terminal bases.

The location of intercalation was confirmed by ^{31}P NMR spectroscopy. The ^{31}P NMR spectrum was assigned from a heteronuclear COSY spectrum.[25,34] Titration of ligand into $d(AGAGCTCT)_2$ gave rise to severe line broadening and shifting of a signal at −1.34 ppm, assigned to P5 (ie, the phosphate in the C^5–T^6 step), and also of signals corresponding to P2, P3, and P6 at −0.84, −1.14, and −1.13 ppm, respectively (Figure 8). These four phosphates are in the G^2–

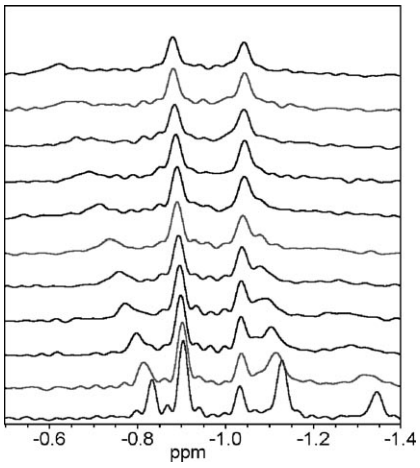

Figure 8. A 1D ^{31}P NMR titration following the addition of $[Ru(tpm)(dppz)(py)]^{2+}$ to $d(AGAGCTCT)_2$. The sequence is shown from bottom to top with each successive spectrum representing the addition of another 0.2 molar equivalents of ligand. From left to right, the signals are from P2; P4 and P7; P1; P6 and P3; and P5.

A^3 and A^3–G^4 steps, implying intercalation in at least one of these two positions. The other three phosphates are affected only to a small extent. A titration with $d(CGAGCTCG)_2$ gave equivalent results.

Structure of the $d(CGAGCTCG)_2$ complex: The structure of the intercalated complex was calculated using a standard restrained molecular dynamics/simulated annealing protocol. However, initial calculations produced complexes in which the ligand was oriented 180° away from the expected orientation, with the dppz ring pointing away from the DNA. This orientation clearly arises because of the lack of intermolecular NOEs involving the dppz ring. Because all the data clearly point to a complex intercalated at the G^2–A^3 step, four additional restraints were added to ensure intercalation, namely from dppz N8 to G^2 N1 and A^3 N1, and from dppz N9 to T^6 N3 and C^7 N3. These additional restraints produced structures in which there were less than half the number of NOE violations, as well as a lower overall RMS violation, and therefore clearly indicate that the experimental data are more compatible with the intercalated structure.

There remained a problem with the calculation, in that the ligand clearly binds in two possible orientations. This was reflected in distorted structures or structures with large NOE violations. The calculation was therefore repeated as an ensemble averaged calculation,[35] in which two independent copies of DNA and ligand were included, and the observed NOEs were required to be satisfied from the ensemble. This calculation reproducibly resulted in both possible orientations of the ligand (Figure 9).

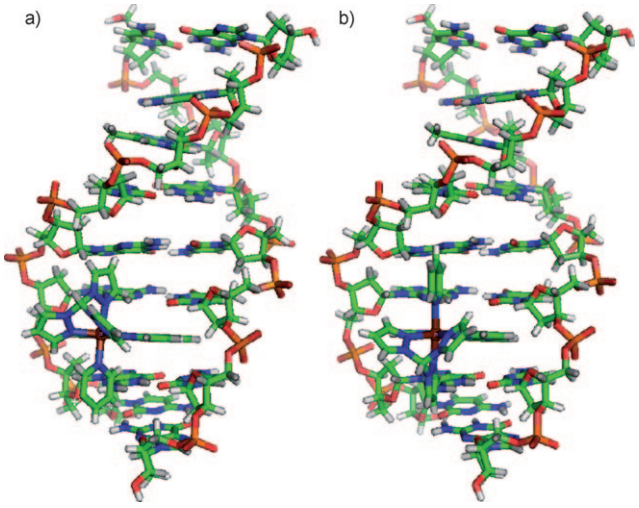

Figure 9. The structure of the complex formed by $[Ru(tpm)(dppz)(py)]^{2+}$ and $d(CGAGCTCG)_2$. Both orientations of the ligand (a and b) are required to satisfy the experimental restraints, although the major conformer is the one shown in (a). The ruthenium atom is in brown.

Ensemble calculations always had some remaining NOE violations, even when carried out using idealized intercalated geometries. We interpret this to indicate that the two geometries shown here, although they satisfy most of the experimental observations, do not represent the entire population of complexes. Calculations came up with a range of alternative geometries, including groove binding and the side-on geometry. It is therefore likely that other conformers such as these are also present in relatively small proportions.

Discussion

As found in previous studies of this and related metallo-intercalators,[7,8,17] measurement of NOEs is hampered by exchange broadening. The solution used here was to measure at elevated temperatures and high nucleotide concentrations, at which the duplex structure is maintained and many protons are in intermediate to fast exchange. However the drawback is that some protons, particularly those of the dppz, are still in slow to intermediate exchange and were too broad to be useful. This means that the number of NOEs used for the structure calculation was limited.

The NMR and spectroscopic data clearly indicate intercalation at the G^2–A^3 step. However, because of the absence of NOEs to the dppz ring, many of the structures calculated had the dppz pointing away from the DNA. Therefore, we added four non-experimental distance restraints in order to ensure intercalation. This means that the depth of intercalation is determined only by the NOEs to the sugar protons. However, since these NOEs hold the complex in the expected position in van der Waals contact with the sugar backbone, we do not believe that the structure is in any way distorted by these non-experimental restraints. This view is supported by the improvement in NOE violations after addition of the extra restraints.

The NMR data indicate that the ligand binds with two possible orientations: a major orientation in which the pyridine axial ligand is pointing toward the end of the double helix, and a minor orientation in which it is pointing toward the center. Both orientations were generated simultaneously using an ensemble averaged calculation.

The structures calculated have the ligand bound in the minor groove, in agreement with the findings of Nordén, Aldrich-Wright, and Collins,[11,12,14–17] but in disagreement with those of Barton.[7–10] The key observation that led Barton et al. to suggest major groove binding was an NOE from dppz to an adenine H8 proton: we concur with Aldrich-Wright and Collins in suggesting that this NOE could also be consistent with minor groove binding. It is, however, clear that the ligand binds in multiple orientations—evidently the two orientations related by a 180° rotation around the dppz long axis described here. It is perfectly possible that different solution conditions may lead the ligand to bind in a completely different orientation, such as coming from the major groove. We note for example that the non-metallic quaternized form of dppz, dqdppz, binds from the major groove.[29]

Here, we have shown that dppz intercalates at the GA step. It is interesting to note that Collins et al.[15,16] also observed sequence specificity for a GA step, while Barton[6] observed binding at either a GT or a GA step. The complex Δ-α-[Rh{(*R*,*R*)-Me_2trien}(phi)]$^{3+}$ binds preferentially at a GC step,[36] while Δ-[Ru(Me_2phen)$_2$(dppz)]$^{2+}$ demonstrates little sequence specificity with a slight preference for being either side of a G,[17] and Δ-[Ru(phen)$_2$(dpq)]$^{2+}$ prefers to bind at a GA step.[14] There is therefore good support for GA as a preferred binding site. It is reasonable to suggest that the preference for G arises from maximization of aromatic stacking interactions.[16]

Our structures have the ligand in a classic head-on perpendicular intercalation geometry. This orientation is dictated by the close van der Waals packing of the ruthenium ligands with the sugar backbone, which makes it difficult to generalize to other ligands. Literature suggests that dppz ligands can intercalate at a wide range of angles, although our study suggests that a side-on geometry leads to poor van der Waals packing, at least for an intercalator as long as dppz. However, a range of angles were observed within the head-on intercalated conformations, which were constrained primarily by van der Waals interactions: see for example Figure 10 below, which shows close steric contact between the DNA and not only the dppz but also pyridine and tpm axial and equatorial rings.

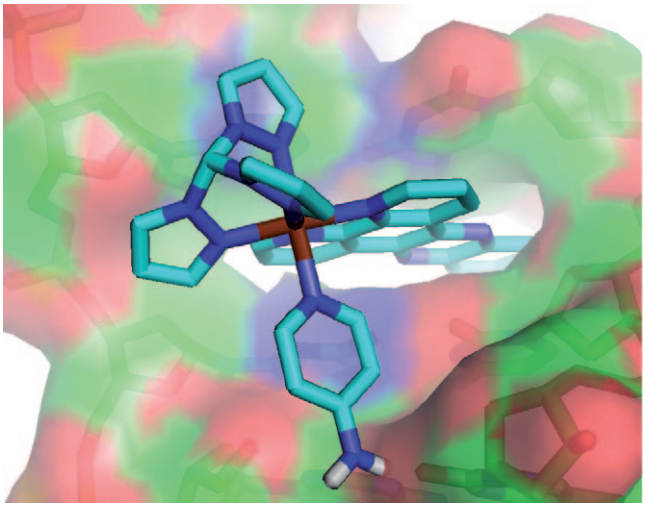

Figure 10. The predicted position of [Ru(tpm)(dppz)(4-NH_2py)]$^{2+}$ bound to DNA. Note the proximity of the 4-amino group to guanine-8 (bottom right): one of the amino protons in this model is only 1.3 Å from G8.

The structures obtained here were for a 2:1 complex of ligand:duplex. Thus, the ligand is in fact intercalated both at the G^2–A^3 step and at the T^6–C^7 step simultaneously, separated by four intervening base pairs. The structure shows that the two ligand molecules are well separated, suggesting that there is no evidence in our experiments for any cooperativity in the binding at multiple sites. Our data therefore here support the conclusions of Barton[37] rather than Nordén.[38]

The optical titrations and viscosity studies reveal that while the [Ru(tpm)(dppz)py]$^{2+}$ cation, together with its 3-aminopyridine derivative, bind with around the same affinity to DNA, the other two complexes—and in particular the 4-NH_2py derivative—display reduced binding affinities. Indeed, it is clear that the 4-aminopyridine derivative does not intercalate into the duplex. This interesting observation can be rationalized using the structural details presented here.

From the NMR structural data it is clear that the 4-H of the coordinated pyridine ligand of [Ru(tpm)(dppz)(py)]$^{2+}$—or any other substituent at the 4 position—is close to the C^1–G^8 base pair, which forms a ledge that protrudes exactly level with the 4-H position, producing steric hindrance to the binding of a 4-substituted pyridine (Figure 10). A similar but even less favorable situation occurs for binding in the opposite orientation (Figure 9b), in which the pyridine is positioned close to the N3 nitrogen of guanine-4 and the sugar backbone. These observations imply that, while substituents on the 3-position of the coordinated pyridine will not greatly exacerbate any unfavorable steric interactions—

as they will be pointing away from the relevant DNA residues—more bulky substitutions in place of the 4-H of pyridine will have a considerably greater effect. This is reflected in the reduced binding affinities of $[Ru(tpm)(dppz)(4\text{-}Mepy)]^{2+}$ and $[Ru(tpm)(dppz)(4\text{-}NH_2py)]^{2+}$ compared to the parent complex and the 3-substituted system. However, since the 4-NH_2py and 4-Mepy ligands are of similar size, a further factor must be invoked to explain the non-intercalation of the $[Ru(tpm)(dppz)(4\text{-}NH_2py)]^{2+}$ ion. It may be that this factor involves electrostatic effects. Although the DFT calculations show that the charge distributions in 4-NH_2py and 4-Mepy complexes are remarkably similar, the absorption and emission spectroscopy changes for the complexes indicate that electrostatic redistribution due to stacking and other noncovalent interactions occur on binding to DNA and this may result in an uniquely unfavorable electrostatic interaction involving $[Ru(tpm)(dppz)(4\text{-}NH_2py)]^{2+}$ and the duplex. However, it seems more likely that the effect is due to the biggest difference between the 4-NH_2py and 4-Mepy complexes revealed by the DFT calculations. The 4-methyl group of $[Ru(tpm)(dppz)(4\text{-}Mepy)]^{2+}$ is a free rotor and can thus rotate to minimize unfavorable steric interactions between the functional group and any closely positioned DNA residue In contrast, the coordinated 4-NH_2py ligand is held rigidly in a position in which intercalation maximizes unfavorable steric interactions (Figure 10), and consequently a groove binding mode becomes more energetically favored. Although steric clashes between the 4-position and G8 could be removed by pulling the dppz some distance out from the DNA, this markedly reduces the steric fit of pyridine and tpm rings to the DNA, and therefore does not improve the affinity for the intercalated geometry. An alternative explanation is that in a groove bound complex the amine group on the pyridine is capable of participating in specific hydrogen bonds in the major or minor groove of DNA and this stabilizes groove binding modes over intercalation.

Conclusions

Using an achiral $\{Ru^{II}(dppz)\}$ building block with a coordination site that can be readily derivatized facilitates the precise positioning of functional groups within a metallo-intercalating system. Using a combination of techniques, including NMR structural studies, it is clear that these systems are minor groove intercalators with a binding preference for GA steps. Furthermore, due to the close contacts made by coordinated ancillary ligands held in the minor groove, the nature and position of a single functional group can greatly modulate the DNA binding properties of the resultant complex and can even entirely "switch off" intercalative binding. These initial results clearly indicate the potential of the $[Ru(tpm)(dppz)(L)]^{n+}$ platform for the construction of systems with modulated binding preferences. In particular, using the structural information gained in this study, derivatives designed to bind to specific and extended sequences will be targeted. The synthesis and characterization of such systems will form the basis of a future report.

Experimental Section

Materials: Oligodeoxyribonucleotides were bought from Sigma–Genosys in a desalted and deprotected form, and were pure by HPLC and mass spectroscopy. By NMR spectroscopy it was evident that although the protecting groups had been cleaved off, they had not been completely removed. However this does not appear to have interfered with the subsequent analysis. $[Ru(tpm)Cl_3]$, $[RuCl(tpm)(dppz)]^+$, and $[Ru(tpm)(dppz)(py)]^{2+}$ were synthesized using previously reported procedures.[24a] Starting materials and solvents were of the highest available purity available from commercial suppliers. All synthetic reactions were carried out under an inert nitrogen atmosphere. The complexes were synthesized and characterized as hexafluorophosphate salts, whilst DNA binding studies were carried out on chloride salts obtained by counter ion metathesis. The buffer used for DNA titrations consisted of 25 mM NaCl and 5 mM tris (pH 7.0) made with doubly distilled water (Millipore). Calf thymus DNA (CT-DNA) was purchased from Sigma and was purified until $A_{260}/A_{280} > 1.9$. Concentrations of CT-DNA solutions were determined spectroscopically using the extinction coefficient of CT-DNA ($\varepsilon = 6600\ dm^3\,mol^{-1}\,cm^{-1}$ at 260 nm).

Instrumentation: UV/Vis spectra were recorded on a Unicam UV2 spectrometer or Cary 50 spectrometer in twin beam mode. Spectra were recorded in matched quartz cells and were baseline corrected. Steady-state luminescence emission spectra were recorded either in aerated acetonitrile or tris buffer solutions on a Hitachi F-4500 instrument. Circular dichroism measurements were carried out on a Jasco Spectropolarimeter at 25 °C. DNA duplex formation is highly sensitive to the concentration of oligonucleotide, and therefore 1.8–2.0 mM oligonucleotide was used, to ensure complete duplex formation. Viscosity measurements were performed on a Cannon-Manning semi-micro viscometer (size 50) immersed in a thermostated bath maintained at 27.0 °C.

Standard ^{1}H NMR spectra were recorded on a Bruker AM250 machine. Binding measurements were carried out using Bruker 500 and 800 MHz spectrometers. Temperatures were calibrated using methanol and ethylene glycol. NMR spectra of free DNA and ligand were assigned at 298 K, while most NMR spectra of the complexes were obtained at 308 K. Standard pulse programs were used, except for the heteronuclear ^{31}P–^{1}H COSY which was adapted from a previous study.[39] The NOESY spectra had mixing times of 100 and 300 ms. Two-dimensional spectra were processed and analyzed in Felix (Accelrys Inc., San Diego, CA).

Computational methods

DFT calculation: Calculations were performed using the SMP version of the Gaussian 03 program package[40] with the B3LYP functional method.[41] Gaussian was compiled using the Portland Compiler version 7.0–5 with the GOTO implementation (v.1.2.6) of BLAS[42] on the EMT64 architecture. In all calculations we used Stuttgart/Dresden pseudo potential[43] on Ru and the D95 V basis set on all other atoms.[44] We initially performed optimizations in vacuo. The converged geometries were used to obtain frequencies in the harmonic approximation. From the optimized geometries we performed additional optimizations, whereby we added solvent effects. The solvent effects were treated by using the polarizable continuum model (PCM)[45] and the united atom topological model[46] applied to radii optimized at the Hartree–Fock 6-31(d) level of theory. This set of radii was used to retain compatibility with the implementation of PCM in earlier versions of Gaussian. We had significant difficulties converging the structures of the molecules, even though each electronic structure step converged quickly. We realized that this was caused by numerical noise in the electronic energies, which in its turn introduced numerical noise in the gradients with respect to changes in the geometry. Based on previous calculations on similar compounds,[47] we changed the standard PCM parameters to OFAC = 0.92 and RMIN = 0.15 to obtain a smoother cavity and better convergence behavior. Unfortunately, this still did not allow for convergence of the geometries. Howev-

er, geometrical energies did converge far enough to obtain qualitative information. All calculations were performed using ultrafine integrals.

Molecular dynamics: Oligonucleotide structure files were prepared using the program nucgen within AMBER 9.[48] Structure files for [Ru(tpm)(dppz)(py)]Cl_2 were created using xplo2d,[49] starting from the crystal structure of the 3-amino pyridine. Energy minimization and restrained molecular dynamics were carried out using XPLOR.[50] Throughout the calculations, planarity of aromatic rings and base pair hydrogen bonding and planarity were maintained, the latter based on the brestraints.inp file in the XPLOR tutorial. Experimental NOEs were classified as strong (1.5–3.5 Å) or weak (2.0–6.0 Å) by comparison to known B-DNA distances.[51] Calculations of complexes started with well-separated B-DNA duplex and ligand, and used energy minimization, followed by MD at 500 K, followed by a gradual exponential cooling over 4000 steps to 100 K, followed by a final energy minimization.[52] During the initial energy minimization, van der Waals radii were gradually increased from zero, to allow the dppz to intercalate. Point restraints were used on atoms within the DNA bases distant from the ligand binding site, to prevent DNA unwinding. Structures were analyzed using the programs Rasmol and pymol.[53]

[Ru(tpm)(dppz)(3-NH_2py)][PF_6]$_2$: [Ru(tpm)(Cl)(dppz)]PF_6 (0.09 g, 0.12 mmol, 1 equiv) and $AgNO_3$ (0.04 g, 0.24 mmol, 2 equiv) were refluxed in ethanol/water (3:1; 40 mL) for five hours. After cooling to room temperature the solution was filtered through celite (to remove solid AgCl). Excess 3-aminopyridine (0.14 g, 1.49 mmol, 12.4 equiv) was added to the solution and the resulting mixture was heated to reflux overnight. After cooling to room temperature the solution was filtered again through celite and aqueous NH_4PF_6 was added. The precipitate was collected by filtration and washed with water, diethyl ether and then dried under vacuum. Mass = 0.072 g (62%) orange solid. ^{1}H NMR ([D_6]DMSO): δ = 5.36 (s, 2H), 6.31 (s, 1H), 6.54 (d, 1H), 6.67 (s, 1H), 6.77 (s, 1H), 6.80 (s, 2H), 8.10 (m, 2H), 8.25 (m, 2H), 8.41 (s, 2H), 8.58 (m, 3H), 8.84 (s, 2H), 9.11 (d, 2H), 9.73 ppm (d, 2H), 10.17 (d, 1H); MS: *m*/*z* (%): 837 (95) [M^+], 691 (100) [M^{2+}], 597 (75) [M^{2+}–(3-NH_2py)]; elemental analysis calcd (%) for $C_{33}H_{26}F_{12}N_{12}P_2Ru\times3H_2O$: C 38.27, H 3.11, N 16.23; found: C 38.69, H 2.53, N 16.23.

[Ru(tpm)(dppz)(4-NH_2py)][PF_6]$_2$: [Ru(tpm)(Cl)(dppz)]PF_6 (0.06 g, 0.08 mmol, 1 equiv) and $AgNO_3$ (0.029 g, 0.17 mmol, 2.1 equiv) were refluxed in ethanol/water (3:1; 40 mL) for five hours. After cooling to room temperature the solution was filtered through celite (to remove AgCl). Excess 4-aminopyridine (0.088 g, 0.93 mmol, 12 equiv) was added to the solution and the resulting mixture was heated to reflux overnight. After cooling to room temperature the solution was filtered again through celite and aqueous NH_4PF_6 was added. The precipitate was collected by filtration and washed with water, diethyl ether and then dried under vacuum. Mass = 0.058 g (76.5%) orange solid. ^{1}H NMR ([D_6]DMSO): δ = 6.15 (d, 2H), 6.25 (m, 1H), 6.55 (s, 2H), 6.75 (d, 2H), 6.80 (d, 1H), 6.90 (m, 2H), 8.10 (dd, 2H), 8.40 (d, 2H), 8.50 (d, 1H), 8.60 (m, 2H), 8.80 (d, 2H), 9.10 (dd, 2H), 9.70 (dd, 2H), 10.05 ppm (s, 1H); MS: *m*/*z* (%): 837 (87) [M^+], 691 (100) [M^{2+}], 597 (56) [M^{2+}–(4-NH_2py)]; elemental analysis calcd (%) for $C_{33}H_{26}F_{12}N_{12}P_2Ru\cdot3H_2O$: C 38.27, H 3.11, N 16.23; found: C 38.19, H 2.55, N 15.85.

[Ru(tpm)(dppz)(4-Mepy)][PF_6]$_2$: [Ru(tpm)(Cl)(dppz)]PF_6 (0.068 g, 0.087 mmol, 1 equiv) and $AgNO_3$ (0.031 g, 0.18 mmol, 2.1 equiv) were refluxed in ethanol/water (3:1; 40 mL) for five hours. After cooling to room temperature the solution was filtered through celite (to remove solid AgCl). Excess 4-picoline (1 mL) was added to the solution and the resulting mixture was heated to reflux overnight. After cooling to room temperature the solution was filtered again through celite and aqueous NH_4PF_6 was added. The precipitate was collected by filtration and washed with water, diethyl ether and then dried under vacuum. Mass = 0.08 g (93.6%) orange solid. ^{1}H NMR ([D_6]acetone): δ = 2.25 (s, 3H), 6.30 (m, 1H), 6.90 (d, 1H), 7.05 (m, 4H), 7.60 (dd, 2H),8.25 (m, 4H), 8.45 (m, 5H), 8.85 (d, 2H), 9.45 (dd, 2H), 9.90 (dd, 2H), 9.95 ppm (s, 1H); MS: *m*/*z* (%): 836 (100) [M^+], 690 (70) [M^{2+}], 597 (60) [M^{2+}–(4-Mepy)]; elemental analysis calcd (%) for $C_{34}H_{27}F_{12}N_{11}P_2Ru\times3H_2O$: C 39.47, H 3.21, N 14.89; found: C 38.62, H 2.39, N 14.45.

X-ray crystallography: X-ray-quality crystals of [Ru(tpm)(dppz)(3-NH_2py)][PF_6]$_2$ were grown from a MeCN/H_2O solvent mixture. Details are available in the Supporting Information. Data were collected on a Bruker SMART diffractometer with an Oxford Cryosystems low-temperature system. Data were collected using graphite-monochromated Mo-Kα radiation (λ = 0.71073 Å) and corrected for Lorentz and polarization effects. Refinement was carried out using SHELXS-97 and SHELXL-97 respectively.[54,55] The structure was solved by Patterson methods and refined by full-matrix least-squares methods on F^2. Hydrogen atoms were placed geometrically and refined with a riding model and the U_{iso} constrained to be 1.2 (1.5 for methyl groups) times U_{eq} of the carrier atom. All non-hydrogen atoms were refined anisotropically. CCDC-733359 contains the supplementary crystallographic data for this paper. These data can be obtained free of charge from The Cambridge Crystallographic Data Centre via www.ccdc.cam.ac.uk/data_request/cif.

Acknowledgements

We thank EPSRC for a DTA studentship (P.W.), and the Wellcome Trust and Biotechnology and Biochemical Research Council for equipment grants. We are grateful for the referees' comments as they have improved the quality of this manuscript. Additionally, J.A.T. is indebted to Dr. Bishwajit Ganguly of the CSMCRI, India for an enlightening conversation.

[1] A. E. Friedman, J. C. Chambron, J. P. Sauvage, N. J. Turro, J. K. Barton, *J. Am. Chem. Soc.* **1990**, *112*, 4960–4962.
[2] R. M. Hartshorn, J. K. Barton, *J. Am. Chem. Soc.* **1992**, *114*, 5919–5925.
[3] E. J. C. Olson, D. Hu, A. Hörmann, A. M. Jonkman, M. R. Arkin, E. D. A. Stemp, J. K. Barton, P. F. Barbara, *J. Am. Chem. Soc.* **1997**, *119*, 11458–11467.
[4] a) B. Önfelt, P. Lincoln, B. Nordén, J. S. Baskin, A. H. Zewail, *Proc. Natl. Acad. Sci. USA* **2000**, *97*, 5708–5713; b) C. G. Coates, J. Olofsson, M. Coletti, J. J. McGarvey, B. Önfelt, P. Lincoln, B. Nordén, E. Tuite, P. Matousek, A. W. Parker, *J. Phys. Chem. B* **2001**, *105*, 12653–12664.
[5] a) M. K. Brennaman, J. H. Alstrum-Acevedo, C. N. Fleming, P. Jang, T. J. Meyer, J. M. Papanikolas, *J. Am. Chem. Soc.* **2002**, *124*, 15094–15098; b) M. K. Brennaman, T. J. Meyer, J. M. Papanikolas, *J. Phys. Chem.* **2004**, *108*, 9938–9944.
[6] G. Pourtois, D. Beljonne, C. Moucheron, S. Schumm, A. Kirsch-De Mesmaeker, R. Lazzaroni, J.-L. Brédas, *J. Am. Chem. Soc.* **2003**, *125*, 683–692.
[7] C. M. Dupureur, J. K. Barton, *J. Am. Chem. Soc.* **1994**, *116*, 10286–10287.
[8] C. M. Dupureur, J. K. Barton, *Inorg. Chem.* **1997**, *36*, 33–43.
[9] R. E. Holmlin, E. D. A. Stemp, J. K. Barton, *Inorg. Chem.* **1998**, *37*, 29–34.
[10] Y. Jenkins, A. E. Friedman, N. J. Turro, J. K. Barton, *Biochemistry* **1992**, *31*, 10809–10816.
[11] E. Tuite, P. Lincoln, B. Nordén, *J. Am. Chem. Soc.* **1997**, *119*, 239–240.
[12] S. D. Choi, M. S. Kim, S. K. Kim, P. Lincoln, E. Tuite, B. Nordén, *Biochemistry* **1997**, *36*, 214–223.
[13] P. Lincoln, A. Broo, B. Nordén, *J. Am. Chem. Soc.* **1996**, *118*, 2644–2653.
[14] I. Greguric, J. R. Aldrich-Wright, J. G. Collins, *J. Am. Chem. Soc.* **1997**, *119*, 3621–3622.
[15] J. G. Collins, A. D. Sleeman, J. R. Aldrich-Wright, I. Greguric, T. W. Hambley, *Inorg. Chem.* **1998**, *37*, 3133–3141.
[16] J. G. Collins, J. R. Aldrich-Wright, I. D. Greguric, P. A. Pellegrini, *Inorg. Chem.* **1999**, *38*, 5502–5509.
[17] A. Greguric, I. D. Greguric, T. W. Hambley, J. R. Aldrich-Wright, J. G. Collins, *J. Chem. Soc. Dalton Trans.* **2002**, 849–855.

[18] P. U. Maheswari, V. Rajendiran, M. Palaniandavar, R. Parthasarathi, V. Subramanian, *J. Inorg. Biochem.* **2006**, *100*, 3–17.
[19] T. Biver, C. Cavazza, F. Secco, M. Venturini, *J. Inorg. Biochem.* **2007**, *101*, 461–469.
[20] C. Hiort, P. Lincoln, B. Nordén, *J. Am. Chem. Soc.* **1993**, *115*, 3448–3454.
[21] I. Haq, P. Lincoln, D. C. Suh, B. Nordén, B. Z. Chowdhry, J. B. Chaires, *J. Am. Chem. Soc.* **1995**, *117*, 4788–4796.
[22] B. M. Zeglis, V. C. Pierre, J. K. Barton, *Chem. Commun.* **2007**, 4549–4696, and references therein.
[23] Y Jenkins, J. K. Barton, *J. Am. Chem. Soc.* **1992**, *114*, 8736–8738.
[24] a) C. Metcalfe, M. Webb, J. A. Thomas, *Chem. Commun.* **2002**, 2026–2027; b) C. Metcalfe, I. Haq, J. A. Thomas, *Inorg. Chem.* **2004**, *43*, 317–323; c) C. Metcalfe, C. Rajput, J. A. Thomas, *J. Inorg. Biochem.* **2006**, *100*, 1314–1319; d) S. P. Foxon, M. Towrie, A. W. Parker, M. Webb, *Angew. Chem.* **2007**, *119*, 3760–3762; *Angew. Chem. Int. Ed.* **2007**, *46*, 3686–3688; e) S. P. Foxon, C. Metcalfe, H. Adams, M. Webb, J. A. Thomas, *Inorg. Chem.* **2007**, *46*, 409–416.
[25] J. D. McGhee, P. H. von Hippel, *J. Mol. Biol.* **1974**, *86*, 469–489.
[26] S. Satyanarayana, J. C. Dabrowiak, J. B. Chaires, *Biochemistry* **1992**, *31*, 9319–9324.
[27] a) C. G. Coates, J. J. McGarvey, P. L. Callaghan, M. Coletti, J. G. Hamilton, *J. Phys. Chem. B* **2001**, *105*, 730–735; b) D. A. Lutterman, A. Chouai, Y. Liu, Y. Sun, C. D. Stewart, K. R. Dunbar, C. Turro, *J. Am. Chem. Soc.* **2008**, *130*, 1163–1170.
[28] a) G. Cohen, H. Eisenberg, *Biopolymers* **1969**, *8*, 45–55; b) L. Kapicak, E. J. Gabbay, *J. Am. Chem. Soc.* **1974**, *96*, 403–408; c) S. Satyanarayana, J. C. Dabrowiak, J. B. Chaires, *Biochemistry* **1993**, *32*, 2573–2584.
[29] P. Waywell, J. A. Thomas, M. P. Williamson, *Org. Biomol. Chem.* in press.
[30] P. E. Schipper, B. Nordén, F. Tjerneld, *Chem. Phys. Lett.* **1980**, *70*, 17–21.
[31] R. Job, P. E. Schipper, *J. Am. Chem. Soc.* **1981**, *103*, 48–51.
[32] F. J. M. van de Ven, C. W. Hilbers, *Eur. J. Biochem.* **1988**, *178*, 1–38.
[33] E. L. Ulrich, H. Akutsu, J. F. Doreleijers, Y. Harano, Y. E. Ioannidis, J. Lin, M. Livny, S. Mading, D. Maziuk, Z. Miller, E. Nakatani, C. F. Schulte, D. E. Tolmie, R. K. Wenger, H. Y. Yao, J. L. Markley, *Nucleic Acids Res.* **2007**, *36*, D402–D408.
[34] A. Pardi, R. Walker, H. Rapoport, G. Wider, K. Wüthrich, *J. Am. Chem. Soc.* **1983**, *105*, 1652–1653.
[35] A. M. J. J. Bonvin, A. T. Brünger, *J. Mol. Biol.* **1995**, *250*, 80–93.
[36] B. P. Hudson, J. K. Barton, *J. Am. Chem. Soc.* **1998**, *120*, 6877–6888.
[37] S. J. Franklin, C. R. Treadway, J. K. Barton, *Inorg. Chem.* **1998**, *37*, 5198–5210.
[38] P. Lincoln, E. Tuite, B. Nordén, *J. Am. Chem. Soc.* **1997**, *119*, 1454–1455.
[39] V. Sklenář, H. Miyashiro, G. Zon, H. T. Miles, A. Bax, *FEBS Lett.* **1986**, *208*, 94–98.
[40] Gaussian 03, Revision C.02, M. J. Frisch, G. W. Trucks, H. B. Schlegel, G. E. Scuseria, M. A. Robb, J. R. Cheeseman, J. A. Montgomery, Jr., T. Vreven, K. N. Kudin, J. C. Burant, J. M. Millam, S. S. Iyengar, J. Tomasi, V. Barone, B. Mennucci, M. Cossi, G. Scalmani, N. Rega, G. A. Petersson, H. Nakatsuji, M. Hada, M. Ehara, K. Toyota, R. Fukuda, J. Hasegawa, M. Ishida, T. Nakajima, Y. Honda, O. Kitao, H. Nakai, M. Klene, X. Li, J. E. Knox, H. P. Hratchian, J. B. Cross, V. Bakken, C. Adamo, J. Jaramillo, R. Gomperts, R. E. Stratmann, O. Yazyev, A. J. Austin, R. Cammi, C. Pomelli, J. W. Ochterski, P. Y. Ayala, K. Morokuma, G. A. Voth, P. Salvador, J. J. Dannenberg, V. G. Zakrzewski, S. Dapprich, A. D. Daniels, M. C. Strain, O. Farkas, D. K. Malick, A. D. Rabuck, K. Raghavachari, J. B. Foresman, J. V. Ortiz, Q. Cui, A. G. Baboul, S. Clifford, J. Cioslowski, B. B. Stefanov, G. Liu, A. Liashenko, P. Piskorz, I. Komaromi, R. L. Martin, D. J. Fox, T. Keith, M. A. Al Laham, C. Y. Peng, A. Nanayakkara, M. Challacombe, P. M. W. Gill, B. Johnson, W. Chen, M. W. Wong, C. Gonzalez, J. A. Pople Gaussian, Inc., Wallingford CT, **2004**.
[41] A. D. Becke, *J. Chem. Phys.* **1993**, *98*, 5648–5652.
[42] K. Goto, R. A. van de Geijn, ACM Transactions on Mathematical Software, 34(3): Article 12; http://www.tacc.utexas.edu/resources/software/software.php. [Last accessed 18 May 2009].
[43] a) A. Nicklass, M. Dolg, H. Stoll, H. Preuss, *J. Chem. Phys.* **1995**, *102*, 8942–8952; b) X. Y. Cao, M. Dolg, *J. Chem. Phys.* **2001**, *115*, 7348–7355, and references therein.
[44] T. H. Dunning Jr, P. J. Hay in *Modern Theoretical Chemistry, Vol. 3* (Ed.: H. F. Schaefer III), Plenum, New York, **1976**, pp. 1–28.
[45] a) B. Mennucci, J. Tomassi, *J. Chem. Phys.* **1997**, *106*, 5151–5158; b) M. Cossi, V. Barone, B. Menucci, J. Tomassi, *Chem. Phys. Lett.* **1998**, *286*, 253–260, and references therein.
[46] V. Barone, M. Cossi, J. Tomassi, *J. Chem. Phys.* **1997**, *107*, 3210–3221.
[47] S. P. Foxon, M. A. H. Alamiry, A. J. H. M. Meijer, I. V. Sazanovich, J. A. Weinstein, J. A. Thomas, unpublished results.
[48] M. Bansal, D. Bhattacharya, B. Ravi, *Bioinformatics* **1995**, *11*, 281–287.
[49] G. J. Kleywegt, *Newsletter Protein Cryst.* **1995**, *31*, 45–50.
[50] X-PLOR version 3.1, A system for X-ray crystallography and NMR, A. T. Brunger, Yale University, Cambridge, **1992**.
[51] D. Neuhaus, M. P. Williamson, *The Nuclear Overhauser Effect in Structural and Conformational Analysis*, 2nd ed., Wiley-VCH, Weinheim, **2000**.
[52] M. Nilges, J. Kuszewski, A. T. Brunger in *Computational Aspects of the Study of Biological Macromolecules by NMR* (Eds.: J. C. Hoch, F. M. Poulsen, C. Redfield), Plenum, New York, **1991**, pp. 451–455.
[53] W. L. DeLano, *The PyMOL Molecular Graphics System*, DeLano Scientific, Palo Alto, **2002**.
[54] SHELXS97 Program for the Solution of Crystal Structure, G. M. Sheldrick, University of Göttingen, Göttingen, **1997**.
[55] SHELXL97 Program for the Refinement of Crystal Structure, G. M. Sheldrick, University of Göttingen, Göttingen, **1997**.

Received: June 25, 2009
Published online: January 27, 2010

